P10.3 HOMOGENEITY PROPERTIES OF RUNWAY VISIBILITY IN FOG AT CHICAGO O'HARE INTERNATIONAL AIRPORT (ORD)

Thomas A. Seliga[1*], David A. Hazen[2] and Stephen Burnley[3]

1. Volpe National Transportation Systems Center, Cambridge, MA
2. Titan/System Resources Corporation, Billerica, MA
3. Federal Aviation Administration, Washington, DC

1. INTRODUCTION

The FAA's forward scatter-based Runway Visual Range (RVR) systems began service in 1994 at several key airports in the U.S and are now used throughout much of the National Airspace System (NAS). Since then, the USDOT Volpe Center has monitored data from a number of airports in order to test RVR system performance. This paper utilizes RVR data collected for this purpose at Chicago O'Hare International Airport (ORD) to assess the spatial homogeneity of RVR conditions during fog events. Previous studies (Seliga et al., 2001; Hazen et al., 2002) provided insights into RVR variability that occurred at three airports (PDX, SEA and ORD); those results showed evidence of strong spatial and temporal variability over the same airport. The criticality of the events (occurrences of Cat II and III conditions) at all three airports was found to often affect only a few of the runways or portions of a runway at a time. These results are consistent with the designated operational need for RVR sensors at touchdown (TD), midway (MP) and rollout (RO) regions of instrumented runways.

In this paper, a statistical analysis of dense fog cases is presented, followed by case studies of a few select events. The latter focuses on visibility measurements from the entire array of sensors along selected runways at ORD and employs comparisons of maximum and minimum measurements from sensors along particular runways as well as comparing measurements from visibility sensors (VSs) at TD and RO with the sensor at MP. The results illustrate that fog events are often highly variable and spatially inhomogeneous. The selection of dense fog events was based on official airport weather METAR reports, that is, events with Category II and III conditions occurring and persisting for at least a few hours.

The insights obtained from this and previous papers on this subject are expected to prove valuable for air traffic planning and lead to more effective operations in the future.

1.1 Terminology

Terms used in this report are defined as follows:

RVR is the range over which a pilot of an aircraft on the center line of a runway can see the surface markings or the lights delineating the runway or identifying its center line. In the US, RVR ranges from 100 - 6,500 ft. Reporting increments are: 100 ft for RVR between 100 - 1,000 ft; 200 ft for RVR between 1,000 - 3,000 ft; and 500 ft from 3,000 - 6,500 ft. Internationally, RVR reports are in m: flexible steps of 25-60 m for RVR up to 800 m; and 100 m for RVR in the 800-1,500 m range (ICAO, 1995).

RVR Visibility Event is defined as any time when RVR is less than 6,500 ft (US) or 1,600 m (international). The most common causes are fog and snow. In the US, the 3 categories of RVR are: Cat I for $2{,}400 \leq \text{RVR} \leq 6{,}500$ ft; Cat II for $1{,}200 \leq \text{RVR} < 2{,}400$ ft; and Cat III for RVR < 1,200 ft.

Although RVR products, reported to controllers, also depend on ambient light intensity and runway light illumination, the values used here are derived solely from extinction coefficient (σ) measurements using VS on active runways. That is, the RVR values are directly derived from σ through Koschmeider's Law for daytime conditions

$$V = 9842.5\ \sigma^{-1} \qquad (1)$$

where V is the visibility in ft and σ is in km^{-1}. This implies σ ranges: from 1.5-4.1 km^{-1} for Cat I conditions; from 4.1-8.2 km^{-1} for Cat II; and over 8.2 km^{-1} for Cat III.

METAR Data Format is the international standard for official reporting of surface weather conditions based on either human observations or automated observing systems. All weather conditions reported in this paper are derived from Automated Surface Observing System (ASOS) METAR data recorded at ORD. METAR visibilities are reported in statute miles (SM). Precipitation and obstruction to visibility are also designated as: SN – snow; BLSN – blowing snow; FG – fog; FZFG – freezing fog; and/or BR – mist.

All times are given in Greenwich Mean Standard Time (GMT). Local standard time at ORD lags GMT by six hours.

2. RVR MEASUREMENTS

Table 1 identifies the VS designations and their respective runway configurations. Note that two of the runways are designated Category III runways with VS located at TD, MP and RO. Four other runways are Category II runways with VS located at each end of the runway. A corresponding map of the runways is shown in Fig. 1. The ASOS site is also identified, since its data are used for generating the METAR reports used here.

* Corresponding Author Address: Thomas A. Seliga, USDOT Volpe Center, 55 Broadway, Cambridge, MA 02142. e-mail: seliga@volpe.dot.gov

Table 1. ORD Visibility Sensor Designations.	
RUNWAY	**VS**
4R22L	VS01 and VS10
4L22R	VS03 and VS11
14R32L	VS04, VS05 and VS06
14L32R	VS07, VS08 and VS09
27R9L	VS03 and VS09
27L9R	VS02 and VS12
18-36	VS11

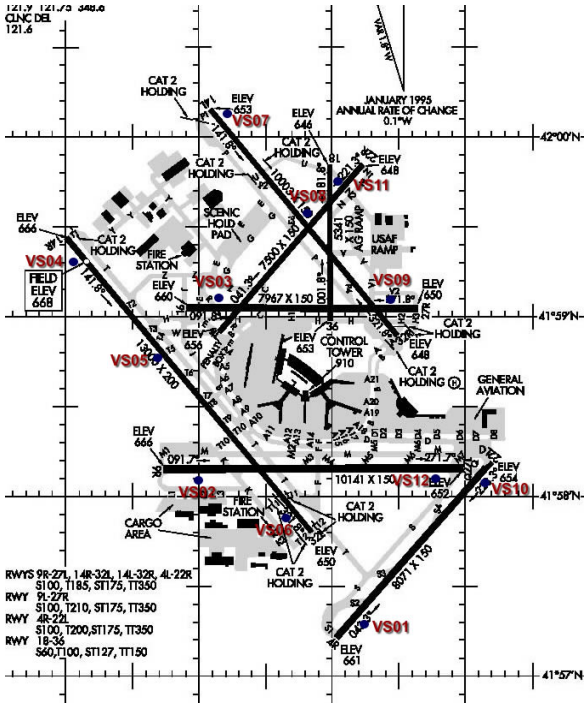

Fig. 1. Runway Map of ORD.

3. GENERAL PROPERTIES

Table 2 lists the fog events selected and considered from the 1998-2000 data. The 'Start Time' and 'End Time' columns in Table 2 are the approximate start and end times in GMT. The 'Max σ' column is the maximum σ measured by any of the VS during the event. The events ranged in duration from about 3¼ to 19½ h, although the events of 1/22/99-1/23/99 could be considered a single event lasting 23 h.

Event Statistics - Table 3 lists the percent of event time individual Category II and III runways, identified by the column headers, were completely in Category III fog conditions. The column 'Dur min' is the duration of the fog event in minutes. This statistic is an indication that spatial homogeneity during severe fog events varies widely from event to event and throughout events. The most consistent events were 3/2/98, 1/23/99 and 12/4/99 in that each runway was completely in Category III fog conditions at least a third of the event duration. Other fairly consistent events occurred on 2/25/00 and 6/1/00. It also should be noted that during less uniform events, Category III fog might occur much less often on one runway than its parallel counterpart.

Table 2. ORD Fog Events.			
DATE	**START TIME**	**END TIME**	**MAX σ**
3/2/98	0830	1145	34
3/18/98	0100	2030	44
5/1/98	0030	1130	31
9/25/98	0700	1530	53
1/17/99	0445	1450	89
1/20/99	0500	1800	57
1/22/99	1230	2355	49
1/23/99	0035	1130	48
12/4/99	0530	1800	45
2/25/00	0300	1730	44
6/1/00	0200	1200	32
8/24/00	0605	1305	37
10/17/00	0600	1200	44
10/25/00	0600	1600	18

Table 3. Percent of Times Runways in Cat 3 Conditions.							
Event Date	**Dur min**	**4R22L**	**4L22R**	**27R9L**	**27L9R**	**14R32L**	**14L32R**
3/2/98	200	41.5	39.0	46.0	48.5	46.5	33.0
3/18/98	1200	4.0	13.0	13.4	13.3	5.8	10.9
5/1/98	675	8.9	13.3	11.3	8.3	5.0	15.3
9/25/98	525	12.2	4.2	11.2	15.0	13.9	3.4
1/17/99	600	0.2	35.3	7.8	0.0	18.0	9.3
1/20/99	775	13.0	38.7	32.5	18.7	15.6	26.6
1/22/99	685	4.1	28.3	18.2	22.9	40.3	16.1
1/23/99	650	53.5	51.2	48.6	52.5	57.4	54.3
12/4/99	745	48.1	59.9	47.7	56.4	56.6	43.2
2/25/00	875	25.7	31.2	33.4	28.3	27.2	33.0
6/1/00	595	22.0	20.7	20.2	17.0	18.3	24.2
8/24/00	420	0.0	15.0	14.0	0.0	1.7	13.3
10/17/00	365	5.2	6.8	6.3	5.5	11.0	3.6
10/25/00	600	6.0	9.3	11.7	10.0	4.3	13.2

Time Series Plots – Temporal sequences of extinction coefficient measurements were generated for each event for all VSs along the Category II and III runways listed in Table 1. These plots frequently show periods of varying duration where one VS was measuring much higher σ than another VS along the same runway. A sample plot is shown in Fig. 2. The lines labeled 'Cat I', 'Cat II' and 'Cat III' are reference levels for the daytime criteria of σ listed in Sect. 1.1. Fig. 2 also shows that the one-min averages for σ can vary greatly and thus may give reported values of visibility that may be non-representative of actual average conditions.

Histograms - The frequency of the ratios of maximum σ to minimum σ for each Category II and III runway and for each event were taken as a means for examining the spatial homogeneity of events. A sample histogram plot (magenta curve) is shown in Fig. 3; the maximum of the distribution is normalized to one for display convenience. Included with the histograms are cumulative distributions (CDF, red curve) and 1-CDF (blue curve) of the ratios of maximum to minimum σ. The intersection of the CDF and the 1-CDF curves locates the median of the ratios.

These latter measures are useful for estimating probabilities of occurrence.

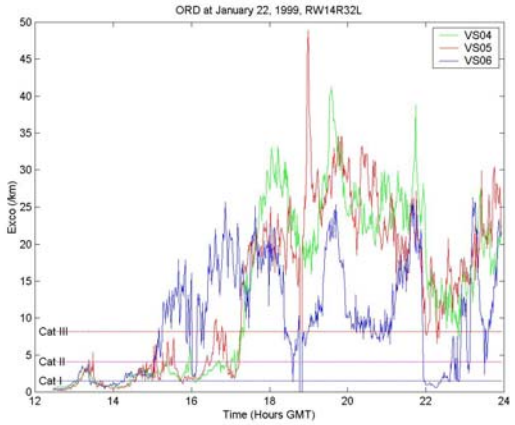

Fig. 2. Sample Time Series Plot.

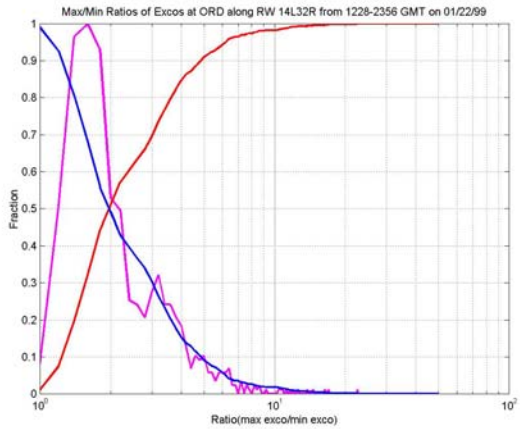

Fig. 3. Sample Histogram and Cumulative Distribution Function Curves of the Max/Min Ratios of Extinction Coefficient from TD, MP and RO Locations.

In general, there was considerable spread in the distributions for most events along a particular runway. The actual maximum frequency for a particular ratio range was typically less than 0.1 for a 0.2 bin size. The ratio where this maximum frequency occurred was frequently far greater than one; the farther this measure is from one, the more inhomogeneous is the fog. The highest actual peak frequency was about 0.2 along RW 27R9L during the March 2, 1998 event at ratios near 1.1; this corresponded to a relatively highly homogeneous fog event. Generally, the distribution for one runway was considerably different than that of any other runway during the same event. The medians of the ratios ranged mostly between ~1.1 to 2.0 with a few values from 2.0-4.9 occurring along one to three runways during: the Jan 17, 1999 event (~4.8 and ~4.9 along RWs 14L32R and 14R32L, respectively, and ~2.3 along RW 27R9L); the Jan 20, 1999 event (~2.2 along RW 14R32L); and the Jan 22, 1999 event (~2.1 and ~2.2 along RWs 14L32R and 14R32L, respectively). It should be noted that when the peak of the distribution tends towards one, the distribution narrows, signifying greater degrees of homogeneity.

Histograms of ratios of σ measurements at TD and RO versus the measurements of σ at MP along the Category III runways (magenta curve) were also produced. A sample plot is shown in Fig. 4. Included again in the histograms are the CDF (red curve) and 1-CDF (blue curve) of ratios of σ.

Again, in many cases, the actual maximum frequency for a particular ratio was typically 0.1 or less. The range of ratios over which the actual frequency was above zero was again very broad, frequently ranging over two orders of magnitude. The median ratios ranged from ~0.4 to ~1.7 with most ratios occurring between ~0.7 to~1.3. Table 4 lists the approximate distances between individual VSs along Category II and III runways.

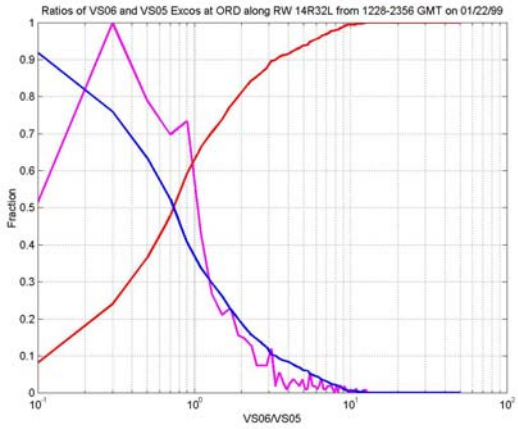

Fig. 4. Sample Histogram of Ratio of TD σ vs MP σ.

Table 4. Distances Between VSs.

RUNWAY	VS PAIR	DIST (ft)
9R27L	02-12	9000
9L27R	03-09	7000
4R22L	01-10	6000
4L22R	03-11	6000
14R32L	06-05	6500
14R32L	05-04	5000
14L32R	09-08	4500
14L32R	08-07	4000

Correlation Distances **–** Plots of the distributions of the maximum ratio of a 'reference' VS such as the VS at MP and another adjacent sensor, such as a VS at TD or RO are used as a tool to assess how often the decorrelation length is less than the separation distance between the two VS. The maximum of the distribution is normalized to one for display convenience. A sample plot is shown in Fig. 5. These plots have a bin width of 0.2 on the maximum ratios plotted on the X-axis. This maximum ratio is defined by $\sigma_{adj}/\sigma_{ref}$, if $\max(\sigma_{ref},\sigma_{adj}) = \sigma_{ref}$ and $\sigma_{ref}/\sigma_{adj}$ if $\max(\sigma_{ref},\sigma_{adj}) = \sigma_{adj}$ where σ_{ref} is the extinction coefficient of the 'reference' VS and σ_{adj} is the extinction coefficient of the adjacent VS. The lower this fraction is,

the more homogeneous the event is between that particular sensor pair. This is determined by obtaining the fraction on the Y-axis where the 1-CDF curve intersects where the maximum σ ratio on the X-axis equals e (~2.718, which implies a natural e^{-1} = 0.368/36.8% homogeneity criterion). To specify different homogeneity criteria, the critical maximum ratio may be set to any other number besides e, e.g., 1.25 would infer a 20% criterion for the homogeneity distance.

This above criterion was used in the events listed in Table 2 for adjacent VS pairs VS05-VS06 and VS05-VS04 along RW 32L14R and for VS pairs VS08-VS09 and VS08-VS07 along RW 32R14L. Eight of the 14 events had fractions defined above <0.1 for the VS05-VS04 comparison; four others were between 0.1-0.19, the remaining two were at 0.25 and 0.26. Only four events had fractions <0.1 at VS05-VS06, which has the longest separation, with five other events between 0.1-0.19; one between 0.2-0.29; three between 0.3-0.39 and one at 0.41. Eleven events had fractions <0.1 for VS08-VS07, which has the shortest separation; with two other events between 0.1-0.19 and one event had a fraction of 0.27. Eight events had fractions <0.1 at VS08-VS09; four other events had fractions between 0.1-0.19; one other event had a fraction of 0.26 and yet another event had a fraction of 0.45. A summary of the results is given in Table 5; note that the lowest average fraction was on the shortest runway and the highest fraction on the longest runway, indicating consistency in the homogeneity properties of the events considered in this analysis.

Table 5. Correlation Statistics

	Average	St Dev	Dist
VS05/VS04	0.111	0.083	5,000
VS05/VS06	0.188	0.118	6,500
VS08/VS07	0.077	0.065	4,000
VS08/VS09	0.129	0.114	4,500

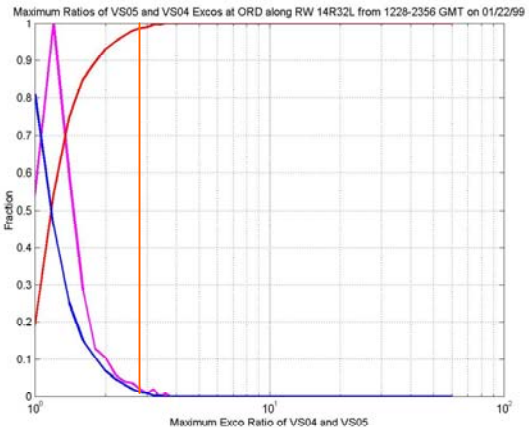

Fig. 5. Sample Histogram and Cumulative Distribution Curves of the Maximum Extinction Coefficient Ratio of a 'Reference' VS and an Adjacent VS.

Scatter Plots - Scatter plots also provide a simple means of examining the homogeneity properties of visibility measured by sensors located different distances from each other. A sample scatter plot is shown in Fig. 6. The blue lines in Fig. 6 define the approximate limits of the spread. The amount of spread depends on the nature of the fog event and the distance between the VS pair analyzed. This example shows that there is tendency for the event to experience poorer visibility conditions at VS04 the spread tends to be less if the distance between a VS pair is relatively short.

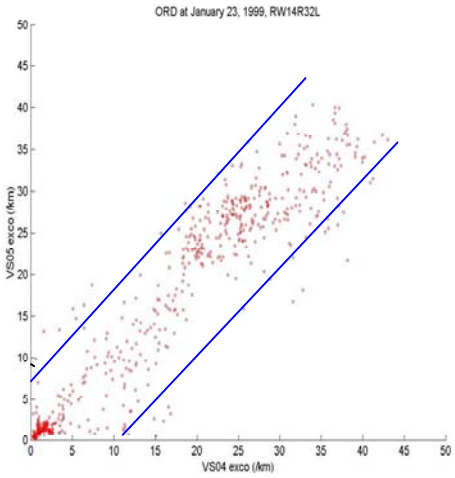

Fig. 6. Sample Scatter Plot.

4. SPECIFIC EVENTS

This section discusses results from three selected fog events. All times are in GMT.

January 22 and 23, 1999 Events – This might be viewed as one event that started at ~1230 on the 22nd and ended at ~1130 on the 23rd. The nature of the fog was different on the 23rd than on the 22nd, however. Peak σ was ~49 km^{-1}.

Weather - The METAR reports indicated 4 SM visibility in mist at 1256 on the 22nd, decreasing to 0.75 SM in mist at 1327 then to 0.5 SM from 1343-1356 in mist and FG. It improved to 0.75 SM from 1432-1447 in mist, then decreased to 0.5 SM at 1456 in FG and to 0.25 SM or less from 1503 on the 22nd to 0122 on the 23rd in FG Visibility was 0.5 SM at 0134 in FG then increased to 1 SM from 0139-0208 in mist, followed by a decrease to 0.25 SM or less from 0221-0856 in FG. Visibility was 0.5 SM from 0956-1107 in mist, then 2 SM at 1131 in mist. Light rain was reported from 2246-2310 on the 22nd, again on the 23rd between 0007-0146, 0740-0956 and from 1107 on past the end of the event.

Reported temperature and dew points were the same throughout the entire two-day event; beginning with 3º C at the start of the event on the 22nd to 1356, then up to 4º C from 1432-1556, up to 5º C from 1656-1811, and then reaching 7º C from 1856-2356. Temperature and dew point were 6º C from 0056-0108 on the 23rd, 7º C from 0122-0139, 8º C at 0156, down to 7º C at 0208 and

6º C from 0221—0356, then back to 7º C from 0456-0556, followed by decreases down to 4º C at 0756-0856 and 3º C from 0956-1131.

The winds remained relatively calm to light throughout the entire event. The wind was from the E to NE from 1156-1656 on the 22nd at speeds ranging from 4-8 kts, then shifted to the SE at 1749, remaining there through 1811 with speeds from 5-7 kts. The wind was SSE from 1856-2156 with speeds of 3-6 kts, and then became light (3-5 kts) with directions between SSW-SE from 2241-0122 and E-SE from 0134-0356 on the 23rd except for 8 kts at 0208. The wind was calm at 0456, then NNE at 3 kts at 0556, then variable wind directions at 3-4 kts from 0756-0823, N-NNE at 5-6 kts from 0856-1131.

Time Series Plots – Fig. 7 shows that VS09 was in Cat I or II visibility conditions while VS07 and VS08 were Cat III along RW 14L32R from about 1710-1810 on the 22nd. Another period from about 1810-2050 showed evidence of all three VSs tracking each other, although they also exhibited significant high frequency variability. Peak readings of σ up to 30 km^{-1} were recorded at ~2120 by VS08. There was a brief lull in the FG along RW 14L32R from ~2200-2310, and then VS07 and VS08 reported higher values of σ after ~2310 through 2359. VS08 did not report higher values of σ until ~2340.

Meanwhile, Fig. 8 shows that, along RW 14R32L, the three VSs tracked reasonably well until ~1500 on the 22nd when VS06 measured considerably higher σ than VS04 or VS05 most of the time from ~1500-1710. VS04 was highest, then VS05 then VS06 from ~1710-1855. VS06 measured significantly lower σ than VS04 or VS05 from ~1815-2115 and again from ~2155-2250 and 2315-2350. A peak σ of ~48 km^{-1} was reported by VS05 at ~1855.

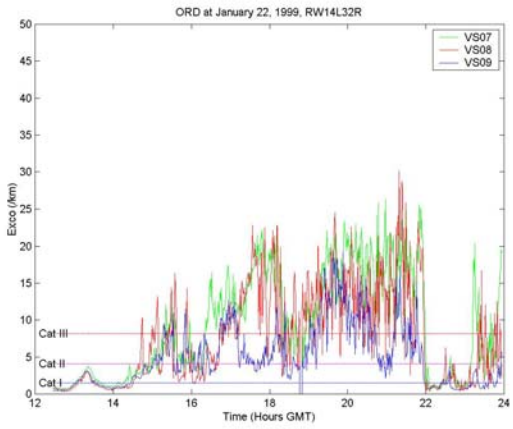

Fig. 7. Time Series along RW 14L32R for 1/22/99 Event.

On the Category II runways, there were periods when one VS recorded a considerably higher σ than the VS on the opposite side of the runway. RW 4R22L reported the lowest σ overall on the 22nd with peaks of ~15 km^{-1} and ~20 km^{-1} recorded at the end of the day. Meanwhile, RW 4L22R recorded σ readings up to ~40 km^{-1} with one VS recording significantly higher σ than the other VS at times. The VSs at RW 4L22R appeared more variable than the VSs at RW 4L22R.

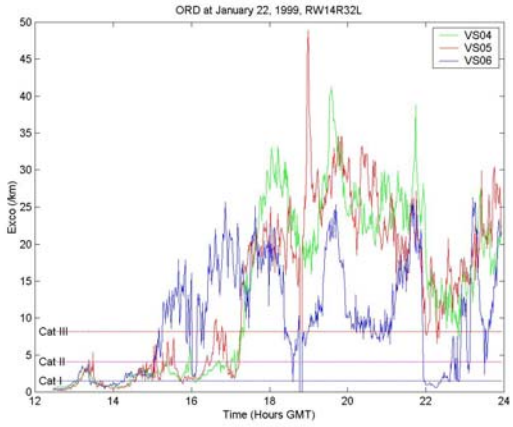

Fig. 8. Time Series along RW 14R32L for 1/22/99 Event.

The FG during the Jan 23, 1999 event was much more consistent than the Jan 22, 1999 event, with Category III conditions recorded by VS04-VS09 from ~0215-0755. Fig. 9 shows a typical time series for this event. This consistency was also evident along the Category II runways.

Histograms - Histograms of the ration of max σ-to-min σ, similar to Fig. 4, show peak frequencies at ratios ranging from ~1.1 to ~1.6 along the Category II and III runways for the Jan 22, 1999 event and ~1.2 to ~1.3 for the Jan 23, 1999 event. Histograms of ratios of VS at an end of the Category III runway to the MP VS show considerably wider range in peaks on the Jan 22, 1999 event than in the Jan 23, 1999 event.

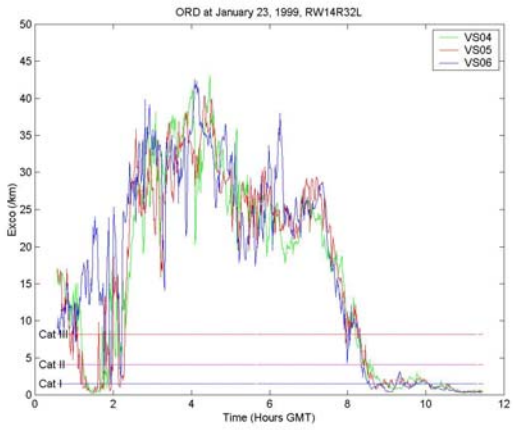

Fig. 9. Time Series along RW 14R32L for 1/23/99 Event.

Correlation Lengths - Inferences about correlation distances may be made from scatter plots of VSs at the ends of the two Category III runways versus the MP VS by comparing the spreads in sensor data relative to the distances between VSs. There was considerably more spread in the VS06-VS05 scatter plot shown in Fig. 10

with 6,500 ft separation than either the VS07-VS08 (4,000 ft) plot shown in Fig. 11 or the VS09-VS08 (4,500 ft) plot (not shown) during both the Jan 22, 1999 and Jan 23, 1999 events. Fig. 12 shows a distinct reduction in the spread occurred for VS07-VS08 on Jan 23, consistent with the premise that the nature of the event differed from the one on the previous day.

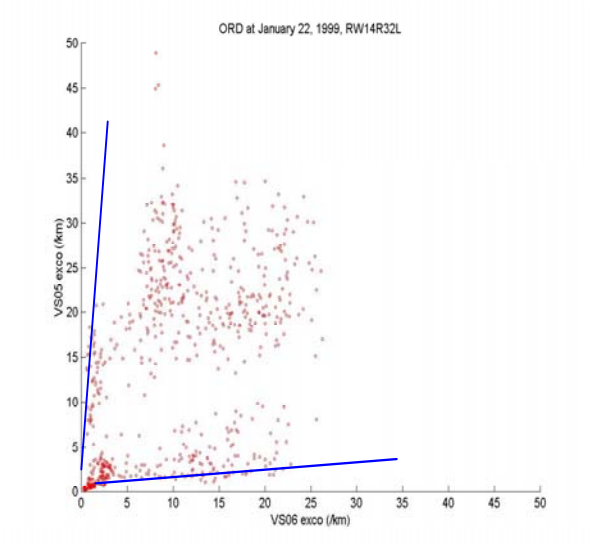

Fig. 10. VS06-VS05 Scatter Plot of 1/22/99 Event (6,500 ft separation).

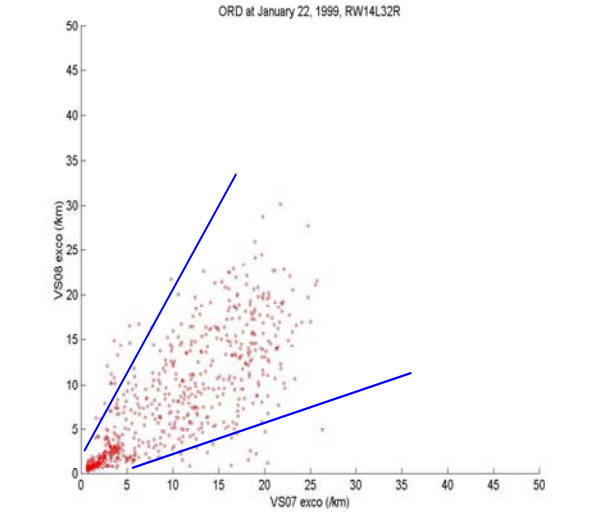

Fig. 11. VS08-VS07 Scatter Plot of 1/22/99 Event (4,000 ft separation).

Maximum extinction coefficient ratio distribution plots similar to Fig. 5 were produced. The results showed that the natural 36.8% homogeneity criterion fraction defined in Sect. 3 was ~0.02 for the VS04/VS05 maximum ratio during the Jan 22, 1999 event, while the sensor pair VS05/VS06 produced a value of ~0.31 for the same event. VS04, VS05 and VS06 are along RW 14R32L. This phenomenon is also seen in the time series plots in Fig. 8, which show VS04 tracking closely with VS05 while VS06 differs considerably from both VS04 and VS05 for large time periods. VS04 and VS05 are about 5,000 ft apart and VS05 and VS06 are about 6,500 ft apart. During this same event, the fractional values (RW 14L32R) VS07/VS08 VS08/VS09 were ~0.09 and ~0.19, respectively. The time series plot shown in Fig. 7 shows that VS07 and VS08 tracked each other well except for high variability of the measurements on short time scales. Note that VS09 tracked considerably lower than VS08 during a significant part of the event when the other two sensors indicated Cat III conditions.

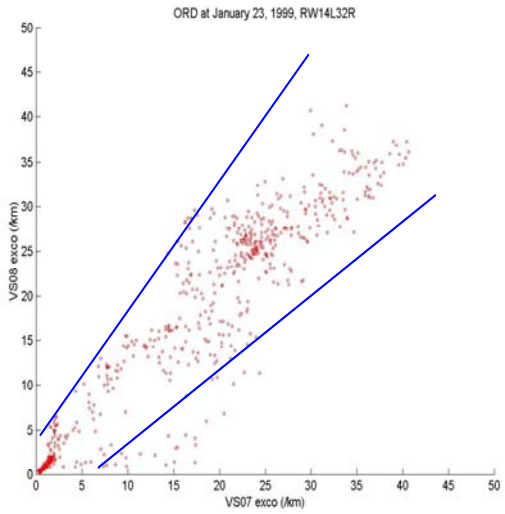

Fig. 12. VS08-VS07 Scatter Plot of 1/23/99 Event (4,500 ft separation).

The maximum extinction coefficient ratio distribution plots (not shown here) for the Jan 23, 1999 event yielded homogeneity criterion fractions of ~0.06 for the VS04/VS05 pair; ~0.05 for the VS07/VS08 pair; ~0.09 for VS05/VS06 pair; and ~0.09 for VS09/VS08 pair. The lower fractions are consistent with the observation that the VSs tracked closer to each other than the Jan 22 event which is further exemplified by comparing the time series plots in Figs. 8 and 9. Comparisons of the results again indicate consistency with the inferences from both scatter plots and histograms.

June 1, 2000 Event – This event began at ~0200 and ended at ~1200 with a peak σ of ~44 km^{-1}.

Weather – The METAR reports indicated 1 SM visibility in mist from 0256-0304, then 0.5 SM in mist at 0317, 2 SM in mist from 0324-0356; decreasing to 0.25 SM or less in mist or FG from 0439-0956, improving to 1.5 SM in mist at 1021 and remaining there until 1056; then 1.25 SM in mist from 1123-1129, 0.75 SM in mist at 1133 and 2 SM in mist at 1156.

Temperatures were 18° C at 0256, 16° C from 0304-0317, 15° C at 0324, 14° C from 0356-0456, 15° C from 0506-0510, 16° C from 0556-1021, 15° C from 1056-1123, 16° C from 1129-1156. Dew points were either the same as the temperatures or a degree less.

There were strong N-NNE winds at 15-20 kts with 24 kts gusts at 0256 and 0304, then NNE at 10-12 kt from 0317-0324, then E at 6 kts, with a 15 kts gust at 0356, The wind speeds were from 3-7 kts from 0456-1056, with wind directions SSE-S from 0456-0556, E at 0616, ESE-SE from 0637-0756, NE at 0856, E from 0956-1021, and SE at 1056. The wind became gusty from 1123-1133, with 18-20 kts gusts recorded with 10-12 kts wind speeds and wind directions from N to NE. Near the end of the event at 1156 the wind blew from the E at 6 kts.

Time Series Plots - Time series plots showed a fairly homogeneous event with RW 4R22L and RW 14L32R showing the best tracking between VSs. Fig. 13 shows the time series along RW 14L32R as typical. VS11 was somewhat higher than VS03 along RW 4L22R for much of the event. VS06 recorded considerably lower σ than VS04 or VS05 from ~0100-0355 and VS04 recorded somewhat lower σ than VS05 or VS06 from ~0430-0555 along RW 14R32L as shown in Fig. 14. The time of densest FG was from ~0400-0600 when all VSs were in Category III FG conditions.

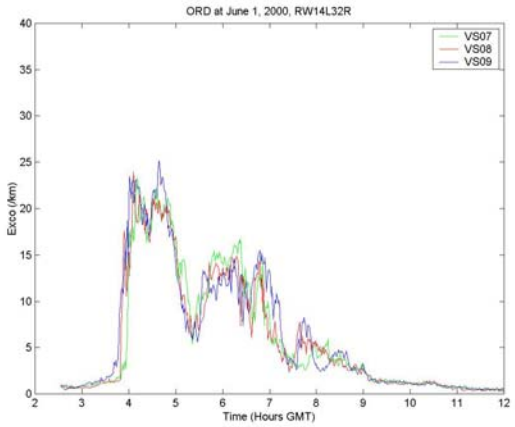

Fig. 13. Time Series of 6/1/00 Event Along RW 14L32R.

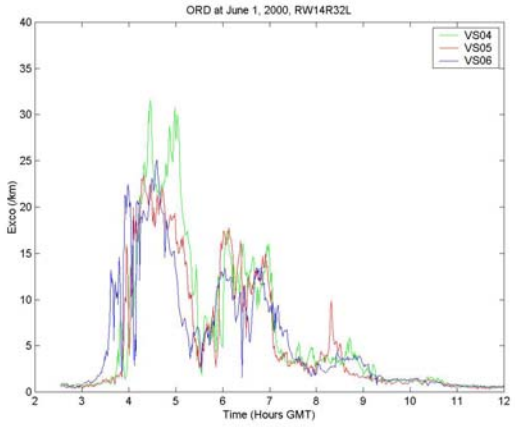

Fig. 14. Time Series of 6/1/00 Event Along RW 14R32L.

Histograms - Histograms of frequencies of ratios of (Max-σ)/(Min-σ) for the Category II and III runways were examined. The plots show ratios peaking between ~1.0-1.3. The distributions were quite narrow, although the ratios ranged over a fairly large range (~1-20) when one of the sensors was experiencing low values of σ. Note that the frequency distributions are again normalized so that maximum frequency is set to one. Figs. 15 and 16 show the distributions along RW 14L32R and RW 14R32L, respectively, to illustrate distribution differences between two parallel runways. Note that the distribution is narrower along RW 14L32R than on RW 14R32L. Comparison between the intersection of the CDF curves with the value of e (2.72), shows that RW 14L32R experienced correlation distances less than the separation distance between sensors around 96% of the time compared to 90% for RW 14R32L.

Histograms of ratios of σ of VS at either end of the Category III runway versus σ at MP were also examined. These are not shown here, but can be used to assess the representativeness of visibility measurements along a runway as determined from a sensor midpoint along the runway.

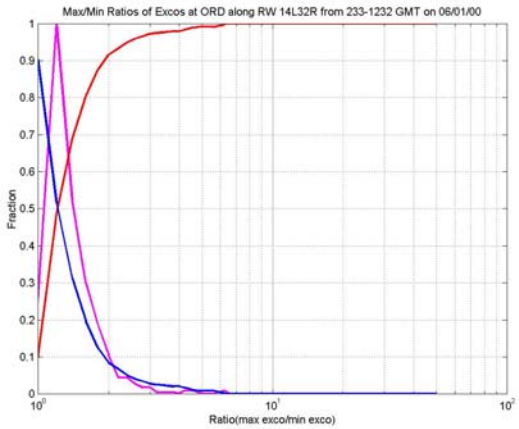

Fig.15. Max-Min Histogram of 6/1/00 Event along RW 14L32R.

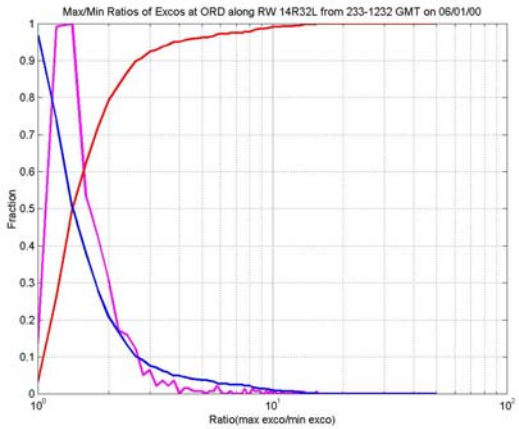

Fig.16. Max-Min Histogram of 6/1/00 Event along RW 14R32L.

Correlation Lengths - Inferences about correlation distances are also made from scatter plots of the VSs at the ends of the two Category III runways vs the MP VS by comparing the spreads against the distances between VSs. There was again considerably more spread in the VS06-VS05 scatter plot shown in Fig. 17 with sensors separated by 6,500 ft compared to the VS07-VS08 (4,000 ft apart) or VS09-VS08 (4,500 ft) plots; the latter plot is shown in Fig. 18. Note also that the spread in results at the longer distance of 6,500 ft separation is broader and more uniform over the range of σ than the spread experienced at the shorter distance of 4,500 ft. Both results also show strong evidence of greater uniformity in visibility at higher visibilities (lower σ) compared to low visibility conditions.

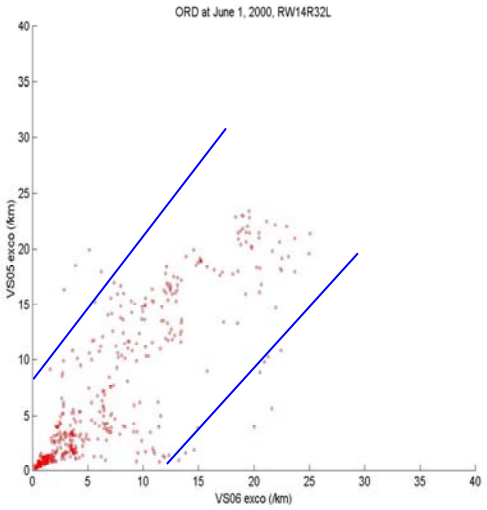

Fig. 17. Scatter Plot of VS06 vs VS05 of 6/1/00 Event.

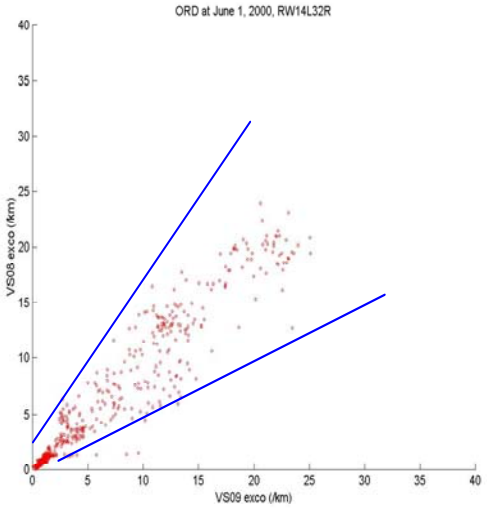

Fig. 18. Scatter Plot of VS09 vs. VS08 of 6/1/00 Event.

Maximum extinction coefficient ratio distribution plots, similar to Fig. 5 (not shown here), shows that the natural 36.8% homogeneity criterion defined in Sect. 3 above demonstrated that the event was quite homogeneous, particularly when compared to the Jan 22, 1999 event. The fraction of times when the correlation distance exceeded the distance between sensors were as follows: VS04/VS05 ~0.03; VS05 / VS06 ~0.06; VS07/VS08 ~0.02; and VS09 / VS08 ~0.01. Consistent with these and the previous histogram results, a comparison of the time series plots in Figs. 13 and 14 show that the VSs tracked quite closely throughout the event. However, the sensors along RW 14L32R (VS07, VS08, VS09) tracked closer to each other than those along RW 14R32L (VS04, VS05, VS06).

5. CONCLUSIONS

This paper examined the spatial homogeneity characteristics of fog (FG) events at ORD The events were selected from the 1998-2000 RVR data archive, identified through an examination of METAR reports on dense fog and corresponding extinction coefficient σ measurements at ORD. Time series plots for each Category II and III runway were examined for differences in σ for each VS along those runways. Histograms of the ratios of max to min σ for each Category II and III runways and ratios of σ from TD and RO VSs to the respective MP VS were examined to assess correlation distances for σ in different events. Scatter plots of σ, comparing values at different VS locations provided additional insight into the homogeneity properties of fog for the events examined here.

Acknowledgements

Leo Jacobs of Titan Corporation and David C. Burnham of Scientific and Engineering Solutions, Inc provided RVR data acquisition and processing assistance.

References

Hazen, D. A., T. A. Seliga, L. Jacobs and P. Narvett, 2002: Visibility variability at the Chicago O'Hare Airport: Insights into the impacts of runway visual range (RVR) measurements on aviation operations, *18th Int. Conf. on Interactive Information and Processing Systems (IIPS) for Meteorology, Oceanography, and Hydrology*, 13-17 Jan, American Meteorological Society.

International Civil Aviation Organization (ICAO), 1995: Meteorological Service for International Air Navigation, Annex 3 to the Convention on International Civil Aviation, 12th Edition.

Seliga, T. A., D. A. Hazen, L. Jacobs and D. B. Lawrence, 2001: Visibility variability at Seattle, WA and Portland, OR: Insights into the impacts of Runway Visual Range (RVR) measurements on aviation operations, *17th Int. Conf. on Interactive Information and Processing Systems (IIPS) for Meteorology, Oceanography, and Hydrology*, 13-18 Jan, American Meteorological Society.